



1 **Atmosphere–ocean exchange of heavy metals and polycyclic**
2 **aromatic hydrocarbons in the Russian Arctic Ocean**

3 Xiaowen Ji^{1,2}, Evgeny Abakumov², Xianchuan Xie^{1*}

4 ¹ *State Key Laboratory of Pollution Control and Resource Reuse, Center for Hydrosocieties Research, School of the*
5 *Environment, Nanjing University, Nanjing 210093, P. R. China*

6 ² *Department of Applied Ecology, Saint Petersburg State University, 16-line, 29, Vasilyevskiy Island, Saint Petersburg*
7 *199178, Russian Federation*

8 * Correspondence: Xianchuan Xie (xchxie@nju.edu.cn)

9



10 **Abstract.** Heavy metals and polycyclic aromatic hydrocarbons (PAHs) can greatly influence biotic activities
and organic sources in the ocean. However, fluxes of these compounds as well as their fate, transport, and net
input in the Arctic Ocean have not been thoroughly assessed. During April–November of the 2016 “Russian
High Latitude Expedition”, 51 air (gases, aerosols, wet deposition) and water samples were collected from the
Russian Arctic within the Barents Sea, Kara Sea, Leptev Sea, and East Siberian Sea. Here, we report on the
15 Russian Arctic assessment of the occurrence in dry and wet deposition of 35 PAHs and 9 metals (Pb, Cd, Cu,
Zn, Fe, Mn, Ni, and Hg), as well as the atmosphere–ocean fluxes of 35 PAHs and Hg⁰. We observed that Hg
was mainly in the gas phase and Pb was most abundant in the gas phase compared with the aerosol and
dissolved water phases. Mn, Fe, Pb, and Zn showed apparently higher levels than the other metals in the three
phases. According to the results for the 35 detected PAHs, the concentrations of PAHs in aerosols and the
20 dissolved water phase were about one magnitude higher than those in gas. The abundances of higher molecular
weight PAHs were highest in the aerosols. Higher levels of both heavy metals and PAHs were observed in the
Barents Sea, Kara Sea, and East Siberian Sea, which were close to areas with urban and industrial sites.
Diagnostic ratios of phenanthrene/anthracene to fluoranthene/pyrene showed a pyrogenic source for the
aerosols and gases, while the patterns for the dissolved water phase were indicative of both petrogenic and
25 pyrogenic sources; pyrogenic sources were most prevalent in the Kara Sea and Leptev Sea. These differences
between air and seawater reflect the different sources of PAHs through atmospheric transport, which included
anthropogenic sources for gases and aerosols and mixtures of anthropogenic and biogenic sources along the
continent in the Russian Arctic. The average dry deposition of \sum_9 metals and \sum_{35} PAHs was 1749 ng m⁻² d⁻¹ and
1108 ng m⁻² d⁻¹, respectively. The average wet deposition of \sum_9 metals and \sum_{35} PAHs was 33.29 μg m⁻² d⁻¹ and
30 221.31 μg m⁻² d⁻¹, respectively. For the atmosphere–sea exchange, the monthly atmospheric input of \sum_{35} PAHs
was estimated at 1040 tonnes. The monthly atmospheric Hg input was approximately 530 tonnes. These
additional inputs of hazardous compounds may be disturbing the biochemical cycles in the Arctic Ocean.

Key words: Trace metals; PAHs; Russian Arctic; atmosphere–water fluxes



35 1 Introduction

The increasing anthropogenic activities associated with growing industries within boundary areas of the Arctic for economic reasons, including hydrocarbon exploration sites and mines in the Russian Arctic, represent potential pollution sources to Arctic ecosystems (Walker et al., 2003; Dahle et al., 2009; Ji et al., 2019). Additionally, the Arctic has long been contaminated by pollutants transported to polar areas from distant locations outside of this region. For example, anthropogenic sources of pollutants in the Arctic have been found to come from the Norilsk industrial area in the Taymyr Peninsula (Reimann et al., 1997; Zhulidov et al., 2011) and from the copper-nickel mining industry in the Kola Peninsula (Boyd et al., 2009; Jaffe et al., 1995). For pollutants transported from outside of the Arctic, reducing global emissions would be an ideal strategy to lessen the impacts of pollutants on Arctic ecosystems. For example, worldwide emissions of mercury will have increased by 25% in 2020 over 2005 levels according to previous estimations (Pacyna et al., 2010), and mercury is a key problematic pollutant in the Arctic. Thus, global emission reductions could help to alleviate problems associated with long-range mercury transport and contamination in the Arctic. In regard to sources close to the Arctic, these may inevitably cause localized ecological risks or risks over a wider regional range. Also of concern is that, with rapid warming of the global climate, the melting of contaminated ice may lead to more pollutant emission into the Arctic Ocean, which could harm its fragile ecosystems.

Pollutants can be transported to the Arctic through both seawater and atmospheric pathways, and the atmospheric pathway is the quickest and most direct way for long-range pollutant transportation, e.g., pollutants can be transported from distant sources to the Arctic within several days or weeks via this pathway (Shevchenko et al., 2003). Reports have revealed that some pollutants such as heavy metals and polycyclic aromatic hydrocarbons (PAHs) can be transported with aerosols over thousands of kilometers to Arctic regions (Rahn and Lowenthal, 1984; Maenhaut et al., 1989; Shaw, 1991; Cheng et al., 1993). Approximately 100 tonnes per year of airborne mercury originating from industrial sources are deposited in the Arctic Ocean (Cone, 2008). While there is evidence that atmospheric inputs make large contributions to the chemical budgets in marine areas, the exact role of these inputs in the Arctic Ocean remains uncertain and may have been previously underestimated (Duce et al., 1991). Numerous studies have proven that aerosol transport is an important way in which atmospheric compounds are transferred from air to ocean water, and this process is susceptible to changes of climate in Arctic regions (Leck et al., 1996; Sirois and Barrie, 1999; Bigg and Leck, 2001). The compounds in aerosols over the Russian Arctic have been reported to show maximal concentrations during the winter/spring season, and 50% of the air pollutants were found to have originated from Russian Arctic pollution itself (Shevchenko et al., 2003). It has also been reported that the natural biodegradation rates of exogenous



compounds in the Arctic Ocean could be lower than those in more temperate oceans such as the Atlantic and Pacific (Bagi et al., 2014). In addition, Vieira et al. (2019) found that some metals (Fe, Mn, and Co) were altered by reductive benthic inputs, and levels were affected by the biological processes of uptake and release in the Arctic Ocean. Because of their toxicity and persistence, high concentrations of heavy metals or other
70 persistent pollutants such as PAHs may disturb the benthic fluxes in cross-shelf mixing in Arctic regions, which could result in adverse effects on marine life, and with the eventual biomagnification in the food web, humans could be affected as well. However, up to now, there has been an insufficient understanding of how these compounds (heavy metals and PAHs) participate in biochemical cycles over the long term in the Arctic Ocean.

The atmosphere–seawater exchange is the major process that controls the residence time and levels of
75 chemical compounds in the Arctic Ocean. In particular, atmospheric deposition is a significant source for pollutants in seawater, and dry deposition in different oceans has been widely studied (Jickells and Baker, 2019; Wang et al., 2019; Park et al., 2019). Although wet deposition (precipitation scavenging) is regarded as playing a predominant role in eliminating pollutants in both gas and particulate phases, current reports on the spatial distribution of pollutants from wet deposition in high-latitude oceans are scarce (Custódio et al., 2014).
80 Moreover, for volatile or semivolatile compounds, the volatilization process is an important pathway for atmosphere–seawater exchanges. Therefore, the atmosphere–water exchange of volatile or semivolatile compounds can be estimated by the net flux of pollutants either volatilizing from seawater to air or depositing from air to seawater (Rasiq et al., 2019; Cheng et al., 2013; Totten et al., 2001). Gonzalez-Gaya et al. (2016) reported on a global assessment of atmosphere–ocean fluxes of 64 PAHs and the net atmospheric PAH input
85 was 0.09 Tg per month to the global ocean. It is undeniable that the atmosphere–seawater exchange rate is greatly influenced by atmospheric temperature variations, and the direction and magnitude of fluxes of compounds between air and seawater vary seasonally (Bamford et al., 1999; Hornbuckle et al., 1994). Additionally, for organic compounds as PAHs, inorganic salt ions can decrease the aqueous solubility of organic compounds (Rasiq et al., 2019). During the period of melting sea ice in the Arctic Ocean, the magnitude and
90 direction of atmosphere–seawater fluxes may be different from those in tropical and subtropical oceans (Gonzalez-Gaya et al., 2016; Rasiq et al., 2019). Although the Arctic Ocean is considered as a sink that receives global airborne pollutants, unfortunately, the characteristics of atmosphere–ocean exchanges of trace metals and organic compounds have remained unclear up to now.

In this study, with the Arctic Ocean as the research area, two categories of pollutants (i.e., 9 heavy metals
95 and 35 PAHs) were measured in aerosols, gas, and seawater, and atmosphere–ocean exchanges of Hg and PAHs were studied. We hypothesized about the relative equilibrium of chemical exchanges between seawater and air



and calculated the net diffusion of atmosphere–ocean exchange of Hg and PAHs in the Arctic Ocean for an evaluation of the double-directional exchange. Meanwhile, the dry and wet deposition of heavy metals and PAHs in the Russian Arctic Ocean were determined. The distributions of heavy metals and PAHs in each sea of the Arctic Ocean and in different phases were also characterized to identify possible sources from the continents.

2 Materials and methods

2.1 Study area and sample collection

All samples were collected during the period of 9th April to 10th November of 2016 as part of the “Russian High Latitude Expedition” carried out on the vessel *Mikhail Somov* (this vessel traveled from the City of Arkhangelsk to Wrangel Island). Fifty-one air and water samples, and eight wet deposition samples were gathered from locations ranging from the southern inlet of the Barents Sea to across the Kara Sea, Laptev Sea, and East Siberian Sea (**Fig. 1**).

2.1.1 Aerosol and gas phase

Air samples, including aerosols and concurrent gases as described elsewhere (Reddy et al., 2012), were collected by a high-volume sampler set up at the top of a main rod. A wind vane was connected to the high-volume sampler so that samples could be collected only if the wind was derived from the bow to prevent contamination from ship emissions. The average sampled air volume was 632 m³ (412–963 m³) per sample. The aerosols were sampled on Teflon filters (P0325-100EA, Fluoropore, Darmstadt, Germany), and then, the compounds in the gas phase were collected over precleaned polyurethane foams (PUFs). After sampling, the filters and PUFs were placed in polyethylene bags, covered with aluminum foil, and frozen at -20 °C prior to chemical analyses.

2.1.2 Wet deposition and water

Wet deposition samples were collected through a cleaned stainless steel funnel connected to a glass bottle during eight snow events. Water samples were gathered continuously from surface seawater (5 m depth) along the vessel, and these samples were immediately filtered onto borosilicate microfiber glass filters (AP1504700, EMD Millipore, Darmstadt, Germany). Then, the compounds in the dissolved phase were retained on XAD sorbent tubes subjected to controlled flows. The mean filtered water volume was 1239 m³ (135–2876 m³). The XAD tubes were stored at 5 °C before their extraction in the laboratory.



125 2.2 Heavy metal extraction and analysis

For the metal determinations in the aerosol, gas phase, wet deposition, and water samples, Teflon filters, PUFs, and dissolved phases were first Soxhlet-extracted for 8 h by using HNO₃, and then, the samples were diluted with deionized water to 23 mL and subjected to inductively coupled plasma mass spectrometry (ICP-MS) analysis. Specifically, the contents of Pb, Cd, Cu, Co, Zn, Fe, Mn, Ni, and Hg were analyzed on an
130 ICP-MS instrument (Thermo Scientific ICE 3500, Waltham, MA, USA) while making use of rhodium (Rh) as an internal standard. High-resolution (10,000) data were collected to avoid any mass interference problems.

2.3 PAH extraction and analysis

For the PAH determinations in the gas, aerosol, and dissolved phase samples, published procedures were used (Berrojalbiz et al., 2011; Castro-Jimenez et al., 2012; Gonzalez-Gaya et al., 2014). Snow-melt water was
135 extracted by using solid phase HLB Oasis cartridges (60 mg/3 cc) on board. Briefly, cartridges were preconditioned with 5 mL methanol, 10 mL of a mixture of methanol:dichloromethane (1:2), and 10 mL deionized water. Afterward, each sample was combined with a recovery standard and concentrated by N₂ until near dryness. Then, it was eluted with 5 mL hexane, 5 mL of a mixture of hexane:dichloromethane (1:2), and 10 mL deionized water.

140 Thirty-five PAH species were quantified, including naphthalene, methylnaphthalene (sum of two isomers), 1,4,5-trimethylnaphthalene, 1,2,5,6-tetramethylnaphthalene, acenaphthylene, acenaphthene, fluorene, dibenzothiophene, anthracene, 9-methylfluorene, 1,7-dimethylfluorene, 9-n-propylfluorene, 2-methyldibenzothiophene, 2,4-dimethyldibenzothiophene, 2,4,7-trimethyldibenzothiophene, 3-methylphenanthrene, 1,6-dimethylphenanthrene, 1,2,9-trimethylphenanthrene,
145 1,2,6,9-tetramethylphenanthrene, fluoranthene, pyrene, benzo[*a*]anthracene, chrysene, 3-methylchrysene, 6-ethylchrysene, 1,3,6-trimethylchrysene, benzo[*b*]fluoranthene, benzo[*k*]fluoranthene, benzo[*a*]pyrene, perylene, dibenzo[*a,h*]anthracene, indeno[1,2,3-*cd*]pyrene, dibenzo[*a,h*]anthracene, and benzo[*g,h,i*]perylene. The PAH quantification was performed with gas chromatography-mass spectrometry (GC-MS). Specifically, we used a gas chromatograph coupled with a triple quadrupole mass selective detector (GS-MS, ITQ 1100,
150 Thermo Scientific, USA) equipped with a DB-5MS chromatographic capillary column (30 m × 0.25 mm i.d. and 0.25-μm film, Agilent Technologies, Santa Clara, CA, USA) operating in electron impact mode (EI) and with selected ion monitoring (SIM) as reported before (Gonzalez-Gaya et al., 2014). The internal standards (anthracene-d₁₀, *p*-terphenyl-d₁₄, pyrene-d₁₀, and benzo[*b*]fluoranthene-d₁₂) were added before operating the GC-MS instrument for the quantification of PAHs, and the recovery of perdeuterated standards
155 (acenaphthene-d₁₀, chrysene-d₁₂, phenanthrene-d₁₀, and perylene-d₁₂) was determined by addition prior to the



procedures of extraction; these values were then used for the correction of measured concentrations.

2.4 Quality assurance and quality control

Analyses of every sample and phase were conducted in the laboratory with field blanks to determine the analytical limits and recoveries. Breakthroughs of aerosols and gas phases were checked for the Teflon filter and PUF samples. Approximately 90% of the metals and PAHs were obtained during the first half of the sample analysis, while the remaining 10% were obtained during the second half; for the PAHs, these mostly consisted of compounds with 2–3 rings. Six blanks (field and laboratory) were collected for the gas phase, while for the dissolved phase, seven field banks and eight laboratory blanks were used, all of which were extracted along with the rest of the samples during the analytical procedure. For the gas phase, average Σ metal values were approximately 0.049 and 0.052 ng per sample in the field and laboratory blanks, respectively, and average Σ PAH values were approximately 2.44 and 2.06 ng per sample in the field and laboratory blanks, respectively (Table S1 and S2, Supplementary material). For the aerosols, average Σ metal values were 0.046 and 0.065 ng per sample in the field and laboratory blanks, respectively, and average Σ PAH values were 2.95 and 2.96 ng per sample in the field and laboratory blanks, respectively. Likewise, for the dissolved phase, values of 0.053 and 0.052 ng per sample were obtained for the Σ metals and values of 2 and 1.73 ng per sample were obtained for the Σ PAHs. All measured PAHs from field samples exceeded the field and laboratory blank concentrations; therefore, the quantified compounds were not subtracted by those values. Mean recoveries of perdeuterated standards used as surrogates in dissolved samples were as follows: 63% for acenaphthene-d₁₀, 54% for chrysene-d₁₂, 73% for phenanthrene-d₁₀, and 82% for perylene-d₁₂.

All concentrations in each medium were corrected by the surrogate recovery for individual samples. The detection limit was used for the lowest limit of the calibration curve. The quantification limit was equivalent to the average blank concentration for each phase.

2.5 Data processing

Dry deposition fluxes (F_{DD} , ng m⁻² d⁻¹) were calculated from field measurements of trace metals and PAHs collected during the expedition over eight time periods. Aerosol deposition fluxes for the metals were calculated as shown in Eq. (1):

$$F_{DD}(\text{metal}) = C_d V_d \quad (1)$$

where C_d is the concentration of atmospheric aerosols and V_d is the velocity of deposition (m s⁻¹). V_d was calculated as shown in Eq. (2), and the details have been described elsewhere (Zhang et al., 2001):

$$V_d = u_{grav} + \frac{1}{R_a + R_s} \quad (2)$$



where u_{grav} is the gravitational settling velocity and R_a and R_s are the aerodynamic resistance for gaseous species and the surface resistance, respectively. R_s can be calculated as follows:

$$R_s = \frac{1}{\varepsilon_0 u_* (E_B E_{IM}) R_1} \quad (3)$$

where ε_0 is an empirical constant ($\varepsilon_0 = 3$) and u_* is the friction velocity calculated for gases. E_B is the collection efficiency of Brownian diffusion as a function of the Schmidt number Sc :

$$E_B = (Sc)^{-\gamma} \quad (4)$$

where γ is an empirical constant ($\gamma = 0.5$). E_{IM} is the collection efficiency from impaction based on the following formulas (Peters and Eiden, 1992):

$$E_{IM} = \left(\frac{st}{0.8 + st} \right)^2 \quad (5)$$

$$st = \frac{V_{\text{grav}} V_*^2}{\nu_a} \quad (6)$$

where ν_a is the kinematic viscosity for air ($\text{m}^2 \text{s}^{-1}$). The correction factor (R_1) is the fraction of particles close to the surface:

$$R_1 = \exp(-st^{1/2}) \quad (7)$$

For PAHs, the specific compound deposition velocity (V_d , cm s^{-1}) was derived from an empirical parameterization (Gonzalez-Gaya et al., 2014):

$$\log(V_d) = -0.261 \log(P_L) + 0.387 U_{10} \text{Chl}_s - 3.082 \quad (8)$$

where P_L is the subcooled liquid vapor pressure of each PAH, U_{10} is the 10 m height wind speed, and Chl_s is the concentration of surface chlorophyll. With Eq. (8), one can estimate the V_d for each PAH and sampling period by taking P_L from references and using the field-measured U_{10} and Chl_s . In this study, $F_{DD}(\text{PAH})$ values were estimated by the measured concentrations of the aerosol phase (C_A , ng m^{-3}) by using

$$F_{DD}(\text{PAHs}) = 864 V_d C_A \quad (9)$$

where 864 is the unit conversion factor.

The wet deposition fluxes (F_w , $\text{ng m}^{-3} \text{d}^{-1}$) of metals/PAHs were estimated by using the quantified concentrations of metals/PAHs from the collected snow and the precipitated volume of snow-melt water per surface and time period for each of the eight snow events during the expedition.

The air–water diffusive fluxes (F_{AW} , $\text{ng m}^{-2} \text{d}^{-1}$) for Hg/PAHs were calculated according to Fick's law:

$$F_{AW} = K_{AW} \left(\frac{C_G}{H'} - 1000 C_{TW} \right) \quad (10)$$

where C_G and C_{TW} represent the concentration measured in the gas phase (ng m^{-3}) and dissolved phase (ng L^{-1}), respectively. H' is the temperature dependence of Henry's law constant, and H' values for PAHs were taken from elsewhere (Bamford et al., 1999); H' for Hg was calculated from Eq. (11) for seawater proposed by



Andersson et al. (2008):

$$H' = \exp\left(\frac{-2404.3}{T} + 6.92\right) \quad (11)$$

where T is the temperature of the surface water (K). H' was corrected by the field-measured salinity. K_{AW} represents the air–water mass transfer rate (m d^{-1}) calculated by a two-film model (Singh and Xu, 1997) and while considering the nonlinear wind-speed effect. C_{TW} for Hg was calculated with directly measured concentrations, and C_{TW} values for PAHs were calculated by using the measured concentrations in the dissolved phase (C_W) as follows:

$$C_T = \left(\frac{C_W}{1 + k_{DOC}DOC}\right) \quad (12)$$

where K_{DOC} was taken as the value of 10% of the octanol–water partitioning coefficient (K_{OW}) (Burkhard, 2000), and DOC represents the dissolved organic carbon (mg L^{-1}).

K_{AW} was calculated by the two-film model:

$$\frac{1}{K_{AW}} = \frac{1}{K_W} + \frac{1}{K_A H'} \quad (13)$$

where K_W and K_A are the mass transfer coefficients (m d^{-1}) of Hg and PAHs in the water and air films, respectively. CO_2 in the water phase of the mass transfer coefficient (K_{W,CO_2} , m d^{-1}) can be used to calculate K_W (Gonzalez-Gaya et al., 2016), which is a wind-speed quadratic function at a height of 10 m (U_{10} , m^{-1}) (Nightingale et al., 2000). A Weibull distribution of wind speed was assumed to parameterize K_{W,CO_2} because average wind speeds were used during the sampling period since the gas and dissolved phase concentrations were averaged values for the sampling transects; K_{W,CO_2} was calculated by using a previously reported method (Livingstone and Imboden, 1993):

$$K_{W,\text{CO}_2} = 0.24\left[0.24\eta^2\Gamma\left(1 + \frac{2}{\xi}\right) + 0.061\eta\Gamma(1 + 1/\xi)\right] \quad (14)$$

where η and ξ are the constants of scale and shape in the Weibull distribution, respectively, and Γ represents a gamma function. $\xi = 2$ (Rayleigh distribution) was used as recommended (Gonzalez-Gaya et al., 2016). η is related to the wind speeds and was calculated with $U_{10} = \eta\Gamma(1 + 1/\xi)$ (Livingstone and Imboden, 1993).

K_W can be calculated by

$$K_W = K_{W,\text{CO}_2} \frac{1}{\sqrt{\frac{SC_{PAH}}{600}}} \quad (15)$$

where SC_{PAH} is the Hg/PAH Schmidt number. The same applies for K_A , which was also calculated on the basis of wind speeds and by using the H_2O mass transfer coefficient for the air phase ($K_{A,\text{H}_2\text{O}}$, cm s^{-1}):

$$K_{A,\text{H}_2\text{O}} = 0.2U_{10} + 0.3 \quad (16)$$

$$K_A = 864K_{A,\text{H}_2\text{O}} \sqrt{\frac{D_{i,a}}{D_{\text{H}_2\text{O},a}}} \quad (17)$$



245 where $D_{i,a}$ and $D_{H_2O,a}$ represent the Hg/PAH and H₂O diffusive coefficients in air, respectively.

The uncertainty was lower than a factor of one to two in these estimates for metals/PAHs. Most of the increasing uncertainty was associated with the Henry's law constants. The effect of uncertainty on the air–water exchange net direction was assessed by the ratios of air–water fugacity (f_G/f_w) (**Fig. S1 and S2, Supplementary material**), and the findings revealed that most metals and PAHs were not close to the
250 equilibrium of air–water. Among the PAHs, net volatilization was detected only for dibenzothiophene, alkylated phenanthrenes, and fluoranthene.

Gross fluxes of volatilization and absorption depend on the first and second term of Eq. (10). The total accumulated fluxes for the Barents Sea, Kara Sea, Laptev Sea, and East Siberian Sea were acquired by multiplying the mean basin flux with the standard deviation by the surface area of each basin.

255 The estimations of degradation fluxes of PAHs in the atmospheric ocean boundary were calculated as follows:

$$D_{atm} = \frac{(C_{Gf} - C_{Gi})ABL}{t} \quad (18)$$

where C_{Gf} and C_{Gi} are the last concentration after a fixed time in a closed system (ng m⁻³) and the concentration in the gas phase at the initial time (ng m⁻³), respectively. t is the time period (average 5 h
260 daytime per day), and ABL represents the average height of the atmospheric boundary layer (380 m). C_{Gf} can be calculated as

$$\ln\left(\frac{C_{Gi}}{C_{Gf}}\right) = k_{OH}[\text{OH}]t \quad (19)$$

where k_{OH} is the rate constant for a PAH reaction with OH radicals (Keyte et al., 2013) and [OH] is the hydroxyl radical concentration in the mixed layer (1000–500 hPa) based on the monthly mean OH radical concentration (Spivakovsky et al., 2000). The mean concentrations of OH were calculated by Eq. (13). The OH
265 concentrations ranged between 5.23 and 17.26×10^5 mol cm⁻³. Besides, only the PAHs in the gas phase were considered while the potential degradation of PAHs bound in aerosols was ignored. Considering the uncertainty of those sources, a relevant error factor of two to three was given in the figure for the degradative fluxes based on the individual PAHs. Because of the large uncertainties in k_{OH} values, the degradation fluxes of PAHs in
270 the atmosphere could not be provided.

3 Results and discussion

3.1 Heavy metals in the atmosphere-ocean

Nine heavy metals were measured, and each metal's average concentration in each sea can be found in



Table S3. The highest \sum_9 metal concentrations in the Barents Sea were found in the gas phase (C_G , ng m^{-3}),
275 where the average concentration was 0.418 ng m^{-3} (**Fig. S3**). The average values of C_G showed no obvious
differences among the four seas, whereas the oceanic area adjacent to the Chukchi Peninsula, Taymyr-Gydan
Peninsula, and Arkhangelsk region showed higher concentrations of the nine metals (**Fig. 2a**). High \sum_9 metal
concentrations in the aerosol phase (C_A , ng m^{-3}) were observed in the Barents Sea ($p < 0.05$), where the average
 \sum_9 metal concentration was 2.713 ng m^{-3} (**Fig. 2b**). These high levels may have been associated with the
280 trajectories of air from the continent of Russia. The distributions of heavy metals in the Russian Arctic Ocean
revealed that the concentrations of the \sum_9 metals in seawater were lower than those in air. The average \sum_9 metal
concentrations in dissolved water (C_W , ng L^{-1}) ranged from 0.526 to $0.896 \mu\text{g L}^{-1}$ (Leptev Sea to Barents Sea).
Obviously higher values of C_W were observed in the Barents Sea–Kara Sea region (Yamal Peninsula) and in the
East Siberian Sea (close to Chukchi Peninsula) in comparison to the C_W values in other areas (**Fig. 2c**).

285 The abundance of each metal in gases, aerosols, and dissolved water is dependent on the emission sources.
In this study, Fe and Zn were the most abundant metals detected in aerosols and dissolved water from the
Russian Arctic Ocean, where the average \sum_9 metal concentrations in aerosols and dissolved water were 0.64 ng
 m^{-3} and 0.91 ng L^{-1} , respectively. Pb was the most abundant metal in the gas phase (the average concentration in
the Russian Arctic Ocean = 0.14 ng m^{-3}). In comparison to aerosols and dissolved water, the gas phase
290 contained higher portions of Hg, which is a finding consistent with the usual form of Hg in the atmosphere
($>98\%$) and the tendency for the remaining types of Hg to adsorb to particles during atmospheric transport
(Poissant et al., 2008). In all phases, the proportions of Mn, Fe, Pb, and Zn were significantly higher than those
of other heavy metals. Additionally, the metal distributions in the Barents Sea and Kara Sea showed the highest
proportions, followed by the metal distributions in the East Siberian Sea. On the Taymyr Peninsula, there is a
295 mining and metallurgical factory operated by the company Norilsk that processes copper and nickel, and it is
one of the biggest metallurgical factories in the world. This may be a likely source of metals in the Kara Sea
region (Shevchenko et al., 2003). Because of the significant differences in the concentrations of metals in the
marine boundary layer both temporally and spatially throughout the Russian Arctic Ocean (Vinogradova and
Polissar, 1995; Shevchenko et al., 1999), as well as the scarcity of reported data on heavy metals in the
300 atmosphere of this region, it was difficult to compare our data with historical findings. However, our data are
similar to those reported in September of 1993 in the Kara Sea (Rovinsky et al., 1995).

The dry deposition flux that involves aerosols binding to heavy metals (F_{DD} , $\text{ng m}^{-2} \text{ d}^{-1}$) is a major process
for heavy metal deposition (Shevchenko et al., 2003). In the Russian Arctic Ocean, the average F_{DD} of the \sum_9
metals ranged from 392 to $8067 \text{ ng m}^{-2} \text{ d}^{-1}$ (mean = $1792 \text{ ng m}^{-2} \text{ d}^{-1}$). The largest F_{DD} value was found close to



305 the coast of the East Siberian Sea, where F_{DD} values of Hg and Pb were dominant and values of 305 and 224 $\text{ng m}^{-2} \text{d}^{-1}$, respectively, were observed (**Fig. 3a**). Our results seem to be one magnitude higher than those in the Red Sea (mean = 615 $\text{ng m}^{-2} \text{d}^{-1}$) (Chen et al., 2008) and Mediterranean Sea (mean = 264 $\text{ng m}^{-2} \text{d}^{-1}$) (Chester et al., 1999). However, this comparison may not reflect the strength of the emission sources because dry deposition is highly dependent on the deposition velocity, which is affected by meteorological conditions such as the humidity, wind speed, and stability of the air column (Mariraj Mohan, 2016). The relative humidity in the Arctic Ocean tends to be higher in coastal areas and notably we sampled during spring–winter when water vapor evaporates from the relatively warmer surfaces of seawater (Vihma et al., 2008). Also, the wind over sampling sites in the Arctic Ocean was approximately 7 m s^{-1} on average (the largest average wind speed was about 9 m s^{-1} in the Barents Sea), which was significantly higher than the wind in the Red Sea and Mediterranean Sea (0.36–1 m s^{-1}) (Chen et al., 2008; Chester et al., 1999). During the eight snow events encountered during the expedition, the wet deposition flux of the \sum_9 metals (F_{WD} , $\mu\text{g m}^{-2} \text{d}^{-1}$) ranged from 23 to 32 $\mu\text{g m}^{-2} \text{d}^{-1}$ (mean = 26 $\mu\text{g m}^{-2} \text{d}^{-1}$) (**Fig. 4a**). Data relevant to the wet deposition flux of heavy metals in the Arctic region include results for Hg, which was estimated on land in Alaska and the highest deposition was detected along the southern and southeastern coasts (exceeding 0.05 $\mu\text{g m}^{-2} \text{d}^{-1}$) (Pearson et al., 2019); the values were quite similar to the F_{WD} for Hg in our results (0.05 to 0.09 $\mu\text{g m}^{-2} \text{d}^{-1}$). Through analysis of variance tests, we did not find any significant difference in the F_{WD} at different locations ($p > 0.05$) for all heavy metals, while a relatively higher F_{WD} for Hg was observed in coastal areas adjacent to the Taymyr Peninsula with industrial factories. Pearson et al. (2019) pointed out that there are larger contributions from Hg wet deposition in the Bering Sea and Gulf of Alaska, which are influenced by the western Pacific downwinds of East Asia, where high Hg emissions from industrial activities and coal burning occur (Wong et al., 2006). The Russian Arctic Ocean is also affected by Pacific downwinds, which could lead to a combination of heavy metal deposition from both local anthropogenic sources and long-range transport from Asia. Wet deposition is an important process for the transfer of heavy metals from gas and aerosol phases to ocean water. Snowfall in the Arctic is an important fraction of precipitation, but variations in measurements ranging from 20% to 50% can occur during windy conditions even with sampling equipment designed with wind protection (Rasmussen et al., 2012). However, snow events are quite sporadic in the Russian Arctic Ocean during spring–summer compared with the other deposition processes. Nevertheless, the wet deposition in our study has relatively high uncertainty and is under regional influences.

For many heavy metals that form volatile species, there is additional evidence that their existence in water is strongly related to releases from terrestrial environments rather than internal cycling in aquatic systems



(Robert, 2013). For example, following the deposition of atmospheric Fe, a non-volatile species, the concentrations in water are influenced mainly by the particulate phase and its dissolution, whereas for Hg, a volatile species that predominantly exists in the atmosphere as a gas (Hg^0), the concentrations of volatile Hg species in water are largely influenced by volatilization and deposition processes at the air–water interface; portions of the Hg in aquatic systems ends up being converted to methylmercury (Mason and Sheu, 2002; Sunderland and Mason, 2007; Selin et al., 2007; Strode et al., 2007). Hg concentrations in the gas phase in the present study were significantly lower than those measured in 1996 in the Northern Hemisphere ($1.5\text{--}1.7\text{ ng m}^{-3}$) and Southern Hemisphere ($1.2\text{--}1.3\text{ ng m}^{-3}$) (Steffen et al., 2005; Slemr et al., 2003; Wängberg et al., 2007; Kim et al., 2005). Steffen et al. (2002) indicated that there has been increasing retention of Hg in the Arctic region based on analyses of long-term measurements of atmospheric Hg concentrations. Diffusive air–water exchange is the dominant process driving the exchange of Hg in the ocean. The net diffusive air–water exchange ($F_{\text{AW}}, \text{ng m}^{-2} \text{d}^{-1}$) was estimated by a two-film resistance model (Robert, 2013). The net input of Hg was calculated as shown in **Fig. 3b**, and the results revealed there was a net input from the atmosphere to the ocean at all stations, especially for the stations close to industrial/urban areas. The integrated monthly F_{AW} fluxes (tonnes per month) for Hg were of the same order of magnitude as the F_{DD} fluxes for Hg and other heavy metals in the Russian Arctic Ocean (**Fig. S4**). For Hg, the gross volatilization and gross absorption in the Russian Arctic Ocean were 250 tonnes per month and 530 tonnes per month, respectively. In consideration of previous studies concerning atmospheric mercury depletion events (AMDEs) during which the net input of Hg in the Arctic was evaluated (Brooks et al., 2006; Lindberg et al., 2001), we adjusted our sampling times to avoid sampling during sunrise when the autocatalytic release of sea salt aerosols changes the oxidative photochemistry in the stratified planetary boundary layer where elemental and reactive Hg in the gas phase is oxidized by reactive halogens. It was estimated that about 99 to 496 tonnes of Hg are deposited per year in the Arctic during AMDEs (Skov et al., 2006; Ariya et al., 2004). The net input of Hg in this study was apparently one order of magnitude higher than that caused by the AMDEs, and this discrepancy may have been related to the fact that the previous studies were estimated based on the terrestrial boundary between air masses and snowpack, and that the different locations and seasons were affected by different meteorological conditions. In northern regions it has been shown that Hg undergoes long-range transport from Eurasia, especially during the winter season (Poissant et al., 2008). These net amounts of Hg entering into the Arctic Ocean pose potential risks to marine biota because Hg is poorly mobile and can be retained by aquatic biota that are exposed to the Hg during the deposition process (Harris et al., 2007).

3.2 PAHs in the atmosphere-ocean



Thirty-five individual PAHs, which included isomer groups such as alkylated PAHs, were measured. The average concentrations of PAHs in each sea of the Russian Arctic Ocean are shown in **Table S4**. The average values of C_G showed no obvious differences in the Kara Sea, Laptev Sea, and East Siberian Sea ($p > 0.05$), and no particularly high levels of C_G were detected at all of the sampling sites (**Fig. 5a**). The highest \sum_{35} PAH concentration in the gas phase (C_G , ng m^{-3}) occurred in the Barents Sea, and the value was 215 ng m^{-3} . PAH concentrations in aerosols (C_A , ng m^{-3}) in the Barents Sea, Kara Sea, and East Siberian Sea were apparently higher than those in the gas phase (**Fig. 5b**) with average C_A values of 215.67, 130.80, and 77.72 ng m^{-3} , respectively. Similar to the pattern for heavy metals mentioned above, these chemicals may have been derived from atmospheric transport from the Russian continent. The average \sum_{35} PAH concentrations in dissolved water (C_W , ng L^{-1}) ranged from 13.12 ng L^{-1} (Laptev Sea) to 60.88 ng L^{-1} (Barents Sea), of which the variability was similar to that of PAH concentrations in aerosols. Higher levels of C_W were also found along the coast of the Yamal-Gydan Peninsula where petrol and natural gas industries have active sites (**Fig. 5c**).

The contribution of each PAH in the gas, aerosol, and dissolved water phases is determined by its source, volatility, and hydrophobicity (Lima et al., 2005). The low-molecular weight PAHs were dominant in gas and dissolved water (**Fig. S5**). In the gas phase, low-molecular weight PAHs occupied more than 75% of the \sum_{35} PAHs, which mainly contained methylated phenanthrenes, e.g., methylphenanthrene (mean = 1.31 ng m^{-3}), dimethylphenanthrene (mean = 1.27 ng m^{-3}), and trimethylphenanthrene (mean = 1.32 ng m^{-3}), and methylated dibenzothiophenes, e.g., methyl dibenzothiophene (mean = 1.29 ng m^{-3}), dimethyl dibenzothiophene (mean = 1.27 ng m^{-3}), and trimethyl dibenzothiophene (mean = 1.32 ng m^{-3}). In dissolved water, methyl naphthalene and tetramethyl naphthalene were the most abundant PAHs with average concentrations of 1.12 and 1.45 ng L^{-1} , respectively. Measured values of C_G , C_A , and C_W are known to vary with the changes of each PAH concentration in the marine environment (Berrojalbiz et al., 2011; Castro-Jimenez et al., 2012; Cabrerizo et al., 2014). However, there were no previous reports about the occurrence of PAHs in the Russian Arctic atmosphere and ocean.

The average dry deposition flux (F_{DD}) of the \sum_{35} PAHs was $1108 \text{ ng m}^{-2} \text{ d}^{-1}$. Dry deposition is a major process for high-molecular weight PAHs bound to aerosols (**Fig. 6a**). The deposition values varied mainly in accordance with the PAH concentrations of aerosols in suspension and the factors influencing the deposition velocities (wind speed, compound vapor pressure, etc.). The wet deposition flux of the \sum_{35} PAHs (F_{WD} , $\text{ng m}^{-2} \text{ d}^{-1}$) ranged from 205 to $241 \mu\text{g m}^{-2} \text{ d}^{-1}$. Wet deposition is an important purging process for semivolatile organic compounds such as PAHs in the gas and aerosol phase. Snow events are quite sporadic in the Arctic Ocean, and thus, these have lower relevance for wet deposition of PAHs in this region.



The estimated net diffusion of air–water exchange (F_{AW} , $\text{ng m}^{-2} \text{d}^{-1}$) revealed that most PAHs had net inputs from the atmosphere to ocean except for the more volatile PAHs such as 2–3 ring PAHs (**Fig. 6b**). This is consistent with previous reports in which the results showed that diffusion during air–water exchange is the main process for transfers of relatively lighter volatile organic compounds in the marine environment (Castro-Jimenez et al., 2012; Jurado et al., 2005). The integrated monthly F_{AW} fluxes (tonnes per month) of 5–6 ring PAHs were comparable to F_{DD} fluxes in the Russian Arctic Ocean, whereas only the East Siberian Sea showed higher levels of dry deposition (**Fig. S6**). In all of the four seas, the F_{AW} fluxes of 3–4 ring PAHs were at the same magnitude as the F_{DD} fluxes. The total volatilization and total adsorption of the \sum_{35} PAHs in the Russian Arctic Ocean amounted to 2600 tonnes per month and 3640 tonnes per month, respectively, and thus, there was a net input of the \sum_{35} PAHs from the atmosphere to marine environment that reached 3276 tonnes, which was 100 times higher than the aerosol-bound \sum_{35} PAHs that underwent dry deposition (estimated at around 30 tonnes per month). In other reports, Gonzalez-Gaya et al. (2016) estimated the global input of PAHs from the atmosphere to ocean to be on the order of 90,000 tonnes per month and Reddy et al. (2012) reported that the input of PAHs to the ocean in the Gulf of Mexico in 2010 after the enormous Deepwater Horizon oil spill was 20,000 tonnes. Such comparisons suggest that the diffusive fluxes in the Russian Arctic Ocean play an important role in the atmosphere–ocean exchange of PAHs, whereas there is a relatively lower input of PAHs to the Russian Arctic Ocean on the global scale.

In addition to the transfers of PAHs to the ocean, PAHs also can be degraded during transport through the atmosphere because of reactions with OH radicals (Keyte et al., 2013). The degradation fluxes (D_{atm} , $\text{ng m}^{-2} \text{d}^{-1}$) of PAHs in the gas phase of the oceanic atmosphere (**Fig. 7**) was estimated at 3000 tonnes per month for the \sum_{35} PAHs, and this represents an additional PAH sink (see Methods). In general, the large amounts of PAHs undergoing net deposition to the ocean and degradation during atmospheric transport must be indicative of large source areas in the Russian Arctic. Notably, PAHs have been increasing in the atmosphere owing to wildfires and fossil fuel use over the past century (Zhang and Tao, 2009). The high-molecular weight PAHs were dominant in the aerosols (**Fig. 5**) originating from pyrolytic sources (Lima et al., 2005). Besides, high abundances of alkylated PAHs were observed in the gas and dissolved phases, and along with the evaluations of the diagnostic ratios (**Fig. S7**), the results were suggestive of pyrogenic sources for PAHs in gases and aerosols, and mixtures of pyrogenic and petrogenic sources for PAHs in dissolved water (mostly for the Leptev Sea and East Siberian Sea). Other sources contributing to the occurrence of PAHs may have involved both anthropogenic and biogenic sources on the land (Cabrerizo et al., 2011). In this region, it can be assumed that PAHs in the atmosphere (gas and aerosol) originated from anthropogenic sources including industrial and urban



activities, while PAHs in the seawater at the sites with relatively less anthropogenic sources, i.e., the Leptev Sea
430 and East Siberian Sea, originated from a mixture of anthropogenic and biogenic sources. This indicates that
atmospheric transport of PAHs derived from anthropogenic activities is the main input pathway for the Arctic
Ocean.

Because PAHs are toxic, these chemicals can have an adverse influence on food webs in marine
ecosystems (Hylland, 2006). In particular, even though PAHs are present at natural background levels in the
435 marine environment, the massive usage of fossil fuels has led to increases in PAH emissions and excessive PAH
concentrations in many marine environments. The present study indicates that are high contributions of
diffusive atmospheric PAHs to the Arctic Ocean, and these chemicals are potentially perturbing the carbon
cycle in the ocean and posing risks to the fragile Arctic marine food webs. Thus, further studies of the impacts
of such chemicals are warranted.

440 **4 Conclusion**

This study presents the occurrence and atmosphere–ocean fluxes of 35 PAHs and 9 heavy metals in the
Arctic Ocean. Dry deposition and wet deposition fluxes of nine heavy metals in aerosols were estimated at
2205 ng m⁻² d⁻¹ and 10.95 µg m⁻² d⁻¹, respectively. The net gross absorption of Hg in the Arctic Ocean was
estimated at 280 tonnes per month. A net input of PAHs from the atmosphere to the Arctic Ocean was observed
445 for most of the PAHs (35 species), especially for the low-molecular weight PAHs. The net atmospheric input of
the 35 PAHs was estimated at 3276 tonnes per month. The current occurrences of semivolatile aromatic
hydrocarbons could have been derived from biogenic sources and anthropogenic sources from continental land
masses, especially for the locations close to industrial areas. These input concentrations of Hg and PAHs
sources may be causing adverse effects on the fragile Arctic marine ecosystems, and this issue warrants further
450 research.

Author contributions. Dr. Xiaowen Ji and Dr. Evgeny Abakumov set up the sampling equipment and
measured the samples, and they analyzed the data. Dr. Xianchuan Xie also helped to collect and analyze the
data. Dr. Xiaowen Ji and Dr. Xianchuan Xie wrote this manuscript.

Competing interests. The authors declare that they have no conflict of interest.

455 **Acknowledgements.** This work was supported by grants from the Russian Foundation for Basic Research
(18-44-890003, 16-34-60010); by a grant from Saint-Petersburg State University titled “Urbanized ecosystems
of the Russian Arctic: dynamics, state and sustainable development”; by the Jiangsu Nature Science Fund



(BK20151378), and by the Fundamental Research Funds for the Central Universities (090514380001).



References

Andersson, M. E., Gårdfeldt, K., Wängberg, I., and Strömberg, D.: Determination of Henry's law constant for elemental mercury, *Chemosphere*, 73, 587-592, 10.1016/j.chemosphere.2008.05.067, 2008.

Ariya, P. A., Dastroor, A. P., Amyot, M., Schroeder, W. H., Barrie, L., Anlauf, K., Raofie, F., Ryzhkov, A., Davignon, D., Lalonde, J., and Steffen, A.: The Arctic: a sink for mercury, *Tellus B: Chemical and Physical Meteorology*, 56, 397-403, 10.3402/tellusb.v56i5.16458, 2004.

Bagi, A., Pampanin, D. M., Lanzén, A., Bilstad, T., and Kommedal, R.: Naphthalene biodegradation in temperate and arctic marine microcosms, *Biodegradation*, 25, 111-125, 10.1007/s10532-013-9644-3, 2014.

Bamford, H. A., Poster, D. L., and Baker, J. E.: Temperature dependence of Henry's law constants of thirteen polycyclic aromatic hydrocarbons between 4 degrees C and 31 degrees C, *Environ. Toxicol. Chem.*, 18, 1905-1912, 10.1897/1551-5028(1999)018<1905:Tdohsl>2.3.Co;2, 1999.

Berrojaltiz, N., Dachs, J., Jose Ojeda, M., Carmen Valle, M., Castro-Jimenez, J., Wollgast, J., Ghiani, M., Hanke, G., and Zaldivar, J. M.: Biogeochemical and physical controls on concentrations of polycyclic aromatic hydrocarbons in water and plankton of the Mediterranean and Black Seas, *Global Biogeochem. Cycles*, 25, 10.1029/2010gb003775, 2011.

Bigg, E. K., and Leck, C.: Properties of the aerosol over the central Arctic Ocean, *Journal of Geophysical Research: Atmospheres*, 106, 32101-32109, 10.1029/1999JD901136, 2001.

Boyd, R., Barnes, S. J., De Caritat, P., Chekushin, V. A., Melezhik, V. A., Reimann, C., and Zientek, M. L.: Emissions from the copper-nickel industry on the Kola Peninsula and at Noril'sk, Russia, *Atmos. Environ.*, 43, 1474-1480, 10.1016/j.atmosenv.2008.12.003, 2009.

Brooks, S. B., Saiz-Lopez, A., Skov, H., Lindberg, S. E., Plane, J. M. C., and Goodsite, M. E.: The mass balance of mercury in the springtime arctic environment, *Geophysical Research Letters*, 33, 10.1029/2005GL025525, 2006.



Burkhard, L. P.: Estimating dissolved organic carbon partition coefficients for nonionic organic chemicals, *Environmental Science & Technology*, 34, 4663-4668, 10.1021/es001269I, 2000.

Cabrerizo, A., Dachs, J., Moeckel, C., Ojeda, M.-J., Caballero, G., Barcelo, D., and Jones, K. C.: Ubiquitous Net Volatilization of Polycyclic Aromatic Hydrocarbons from Soils and Parameters Influencing Their Soil-Air Partitioning, *Environmental Science & Technology*, 45, 4740-4747, 10.1021/es104131f, 2011.

Cabrerizo, A., Galban-Malagon, C., Del Vento, S., and Dachs, J.: Sources and fate of polycyclic aromatic hydrocarbons in the Antarctic and Southern Ocean atmosphere, *Global Biogeochem. Cycles*, 28, 1424-1436, 10.1002/2014gb004910, 2014.

Castro-Jimenez, J., Berrojalbiz, N., Wollgast, J., and Dachs, J.: Polycyclic aromatic hydrocarbons (PAHs) in the Mediterranean Sea: Atmospheric occurrence, deposition and decoupling with settling fluxes in the water column, *Environ. Pollut.*, 166, 40-47, 10.1016/j.envpol.2012.03.003, 2012.

Chen, Y., Paytan, A., Chase, Z., Measures, C., Beck, A. J., Sañudo-Wilhelmy, S. A., and Post, A. F.: Sources and fluxes of atmospheric trace elements to the Gulf of Aqaba, Red Sea, *Journal of Geophysical Research: Atmospheres*, 113, 10.1029/2007JD009110, 2008.

Cheng, J.-O., Ko, F.-C., Lee, C.-L., and Fang, M.-D.: Air-water exchange fluxes of polycyclic aromatic hydrocarbons in the tropical coast, Taiwan, *Chemosphere*, 90, 2614-2622, 10.1016/j.chemosphere.2012.11.020, 2013.

Cheng, M. D., Hopke, P. K., Barrie, L., Rippe, A., Olson, M., and Landsberger, S.: Qualitative determination of source regions of aerosol in Canadian high Arctic, *Environmental Science & Technology*, 27, 2063-2071, 10.1021/es00047a011, 1993.

Chester, R., Nimmo, M., and Preston, M. R.: The trace metal chemistry of atmospheric dry deposition samples collected at Cap Ferrat: a coastal site in the Western Mediterranean, *Mar. Chem.*, 68, 15-30, doi.org/10.1016/S0304-4203(99)00062-6, 1999.

Cone, M.: *Silent Snow: The Slow Poisoning of the Arctic*, Paw Prints, 2008.



Custódio, D., Cerqueira, M., Fialho, P., Nunes, T., Pio, C., and Henriques, D.: Wet deposition of particulate carbon to the Central North Atlantic Ocean, *Sci. Total Environ.*, 496, 92-99, 10.1016/j.scitotenv.2014.06.103, 2014.

Dahle, S., Savinov, V., Carroll, J., Vladimirov, M., Ivanov, G., Valetova, N., Gaziev, Y., Dunaev, G., Kirichenko, Z., Nikitin, A., Petrenko, G., Polukhina, A., Kalmykov, S., Aliev, R., and Sabodina, M.: A return to the nuclear waste dumping sites in the Bays of Novaya Zemlya, 2009.

Duce, R. A., Liss, P. S., Merrill, J. T., Atlas, E. L., Buat-Menard, P., Hicks, B. B., Miller, J. M., Prospero, J. M., Arimoto, R., Church, T. M., Ellis, W., Galloway, J. N., Hansen, L., Jickells, T. D., Knap, A. H., Reinhardt, K. H., Schneider, B., Soudine, A., Tokos, J. J., Tsunogai, S., Wollast, R., and Zhou, M.: The atmospheric input of trace species to the world ocean, *Global Biogeochem. Cycles*, 5, 193-259, 10.1029/91GB01778, 1991.

Gonzalez-Gaya, B., Zuniga-Rival, J., Ojeda, M.-J., Jimenez, B., and Dachs, J.: Field Measurements of the Atmospheric Dry Deposition Fluxes and Velocities of Polycyclic Aromatic Hydrocarbons to the Global Oceans, *Environmental Science & Technology*, 48, 5583-5592, 10.1021/es500846p, 2014.

Gonzalez-Gaya, B., Fernandez-Pinos, M.-C., Morales, L., Mejanelle, L., Abad, E., Pina, B., Duarte, C. M., Jimenez, B., and Dachs, J.: High atmosphere-ocean exchange of semivolatile aromatic hydrocarbons, *Nature Geoscience*, 9, 438-+, 10.1038/ngeo2714, 2016.

Harris, R. C., Rudd, J. W. M., Amyot, M., Babiarz, C. L., Beaty, K. G., Blanchfield, P. J., Bodaly, R. A., Branfireun, B. A., Gilmour, C. C., Graydon, J. A., Heyes, A., Hintelmann, H., Hurley, J. P., Kelly, C. A., Krabbenhoft, D. P., Lindberg, S. E., Mason, R. P., Paterson, M. J., Podemski, C. L., Robinson, A., Sandilands, K. A., Southworth, G. R., St. Louis, V. L., and Tate, M. T.: Whole-ecosystem study shows rapid fish-mercury response to changes in mercury deposition, *Proceedings of the National Academy of Sciences*, 104, 16586, 10.1073/pnas.0704186104, 2007.

Hornbuckle, K. C., Jeremiason, J. D., Sweet, C. W., and Eisenreich, S. J.: Seasonal Variations in Air-Water Exchange of Polychlorinated Biphenyls in Lake Superior, *Environmental Science & Technology*, 28,



1491-1501, 10.1021/es00057a018, 1994.

Hylland, K.: Polycyclic Aromatic Hydrocarbon (PAH) Ecotoxicology in Marine Ecosystems, *Journal of Toxicology and Environmental Health, Part A*, 69, 109-123, 10.1080/15287390500259327, 2006.

Jaffe, D., Cerundolo, B., Rickers, J., Stolzberg, R., and Baklanov, A.: Deposition of sulfate and heavy-metals on the Kola-Peninsula, *Sci. Total Environ.*, 160-61, 127-134, 10.1016/0048-9697(95)04350-a, 1995.

Ji, X., Abakumov, E., and Polyakov, V.: Assessments of pollution status and human health risk of heavy metals in permafrost-affected soils and lichens: A case-study in Yamal Peninsula, Russia Arctic AU - Ji, Xiaowen, *Human and Ecological Risk Assessment: An International Journal*, 1-18, 10.1080/10807039.2018.1490887, 2019.

Jickells, T. D., and Baker, A. R.: Atmospheric Transport and Deposition of Particulate Matter to the Oceans, in: *Encyclopedia of Ocean Sciences (Third Edition)*, edited by: Cochran, J. K., Bokuniewicz, H. J., and Yager, P. L., Academic Press, Oxford, 21-25, 2019.

Jurado, E., Jaward, F., Lohmarm, R., Jones, K. C., Simo, R., and Dachs, J.: Wet deposition of persistent organic pollutants to the global oceans (vol 39, pg 2426, 2005), *Environmental Science & Technology*, 39, 4672-4672, 10.1021/es050660+, 2005.

Keyte, I. J., Harrison, R. M., and Lammel, G.: Chemical reactivity and long-range transport potential of polycyclic aromatic hydrocarbons – a review, *Chem. Soc. Rev.*, 42, 9333-9391, 10.1039/C3CS60147A, 2013.

Kim, K.-H., Ebinghaus, R., Schroeder, W. H., Blanchard, P., Kock, H. H., Steffen, A., Froude, F. A., Kim, M.-Y., Hong, S., and Kim, J.-H.: Atmospheric Mercury Concentrations from Several Observatory Sites in the Northern Hemisphere, *Journal of Atmospheric Chemistry*, 50, 1-24, 10.1007/s10874-005-9222-0, 2005.

Leck, C., Bigg, E. K., Covert, D. S., Heintzenberg, J., Maenhaut, W., Nilsson, E. D., and Wiedensohler, A.: Overview of the atmospheric research program during the International Arctic Ocean Expedition of 1991 (IAOE-91) and its scientific results, *Tellus B*, 48, 136-155, 10.1034/j.1600-0889.1996.t01-1-00002.x, 1996.



Lima, A. L. C., Farrington, J. W., and Reddy, C. M.: Combustion-Derived Polycyclic Aromatic Hydrocarbons in the Environment—A Review, *Environmental Forensics*, 6, 109-131, 10.1080/15275920590952739, 2005.

Lindberg, S. E., Brooks, S., Lin, C. J., Scott, K., Meyers, T., Chambers, L., Landis, M., and Stevens, R.: Formation of Reactive Gaseous Mercury in the Arctic: Evidence of Oxidation of Hg⁰ to Gas-Phase Hg-II Compounds after Arctic Sunrise, *Water, Air and Soil Pollution: Focus*, 1, 295-302, 10.1023/A:1013171509022, 2001.

Livingstone, D. M., and Imboden, D. M.: The nonlinear influence of wind-speed variability on gas transfer in lakes *Tellus Series B-Chemical and Physical Meteorology*, 45, 275-295, 10.1034/j.1600-0889.1993.t01-2-00005.x, 1993.

Maenhaut, W., Cornille, P., Pacyna, J. M., and Vitols, V.: Trace element composition and origin of the atmospheric aerosol in the Norwegian arctic, *Atmospheric Environment* (1967), 23, 2551-2569, 10.1016/0004-6981(89)90266-7, 1989.

Mariraj Mohan, S.: An overview of particulate dry deposition: measuring methods, deposition velocity and controlling factors, *International Journal of Environmental Science and Technology*, 13, 387-402, 10.1007/s13762-015-0898-7, 2016.

Mason, R. P., and Sheu, G.-R.: Role of the ocean in the global mercury cycle, *Global Biogeochem. Cycles*, 16, 40-41-40-14, 10.1029/2001GB001440, 2002.

Nightingale, P. D., Liss, P. S., and Schlosser, P.: Measurements of air-sea gas transfer during an open ocean algal bloom, *Geophysical Research Letters*, 27, 2117-2120, 10.1029/2000gl011541, 2000.

Pacyna, E. G., Pacyna, J. M., Sundseth, K., Munthe, J., Kindbom, K., Wilson, S., Steenhuisen, F., and Maxson, P.: Global emission of mercury to the atmosphere from anthropogenic sources in 2005 and projections to 2020, *Atmos. Environ.*, 44, 2487-2499, 10.1016/j.atmosenv.2009.06.009, 2010.

Park, G.-H., Lee, S.-E., Kim, Y.-i., Kim, D., Lee, K., Kang, J., Kim, Y.-H., Kim, H., Park, S., and Kim,



T.-W.: Atmospheric deposition of anthropogenic inorganic nitrogen in airborne particles and precipitation in the East Sea in the northwestern Pacific Ocean, *Sci. Total Environ.*, 681, 400-412, 10.1016/j.scitotenv.2019.05.135, 2019.

Pearson, C., Howard, D., Moore, C., and Obrist, D.: Mercury and trace metal wet deposition across five stations in Alaska: controlling factors, spatial patterns, and source regions, *Atmos. Chem. Phys.*, 19, 6913-6929, 10.5194/acp-19-6913-2019, 2019.

Peters, K., and Eiden, R.: Modelling the dry deposition velocity of aerosol particles to a spruce forest, *Atmospheric Environment. Part A. General Topics*, 26, 2555-2564, 10.1016/0960-1686(92)90108-W, 1992.

Poissant, L., Zhang, H. H., Canário, J., and Constant, P.: Critical review of mercury fates and contamination in the arctic tundra ecosystem, *Sci. Total Environ.*, 400, 173-211, 10.1016/j.scitotenv.2008.06.050, 2008.

Rahn, K. A., and Lowenthal, D. H.: Elemental traces of distant regional pollution aerosols *Science*, 223, 132-139, 10.1126/science.223.4632.132, 1984.

Rasiq, K. T., El-Maradny, A., Orif, M., Bashir, M. E., and Turki, A. J.: Polycyclic aromatic hydrocarbons in two polluted lagoons, eastern coast of the Red Sea: Levels, probable sources, dry deposition fluxes and air-water exchange, *Atmospheric Pollution Research*, 10, 880-888, doi.org/10.1016/j.apr.2018.12.016, 2019.

Rasmussen, R., Baker, B., Kochendorfer, J., Myers, T., Landolt, S., Fischer, A., Black, J., Thériault, J., Kucera, P., Gochis, D., Smith, C., Nitu, R., Hall, M., Cristanelli, S., and Gutmann, A.: How well are we measuring snow: the NOAA/FAA/NCAR winter precipitation test bed, 2012.

Reddy, C. M., Arey, J. S., Seewald, J. S., Sylva, S. P., Lemkau, K. L., Nelson, R. K., Carmichael, C. A., McIntyre, C. P., Fenwick, J., Ventura, G. T., Van Mooy, B. A. S., and Camilli, R.: Composition and fate of gas and oil released to the water column during the Deepwater Horizon oil spill, *Proceedings of the National Academy of Sciences of the United States of America*, 109, 20229-20234, 10.1073/pnas.1101242108, 2012.

Reimann, C., Boyd, R., deCaritat, P., Halleraker, J. H., Kashulina, G., Niskavaara, H., and Bogatyrev, I.:



Topsoil (0-5 cm) composition in eight arctic catchments in northern Europe (Finland, Norway and Russia), *Environ. Pollut.*, 95, 45-56, 10.1016/s0269-7491(96)00102-9, 1997.

Robert, P. M.: Trace Metals in Freshwaters, in: *Trace Metals in Aquatic Systems*, 2013.

Rovinsky, F., Pastukhov, B., Bouyvolov, Y., and Burtseva, L.: Present day state of background pollution of the natural environment in the Russian Arctic in the region of the Ust-Lena Reserve, *Sci. Total Environ.*, 160-161, 193-199, 10.1016/0048-9697(95)04356-6, 1995.

Selin, N. E., Jacob, D. J., Park, R. J., Yantosca, R. M., Strode, S., Jaeglé, L., and Jaffe, D.: Chemical cycling and deposition of atmospheric mercury: Global constraints from observations, *Journal of Geophysical Research: Atmospheres*, 112, 10.1029/2006JD007450, 2007.

Shaw, G. E.: Aerosol chemical components in Alaska air masses 1. Aged pollution, *Journal of Geophysical Research-Atmospheres*, 96, 22357-22368, 10.1029/91jd02058, 1991.

Shevchenko, V., Lisitzin, A., Vinogradova, A., and Stein, R.: Heavy metals in aerosols over the seas of the Russian Arctic, *Sci. Total Environ.*, 306, 11-25, 10.1016/S0048-9697(02)00481-3, 2003.

Shevchenko, V. P., Lisitzin, A. P., Stein, R., Serova, V. V., Isaeva, A. B., and Politova, N. V.: The Composition of the Coarse Fraction of Aerosols in the Marine Boundary Layer over the Laptev, Kara and Barents Seas, in: *Land-Ocean Systems in the Siberian Arctic: Dynamics and History*, edited by: Kassens, H., Bauch, H. A., Dmitrenko, I. A., Eicken, H., Hubberten, H.-W., Melles, M., Thiede, J., and Timokhov, L. A., Springer Berlin Heidelberg, Berlin, Heidelberg, 53-58, 1999.

Singh, V. P., and Xu, C. Y.: Evaluation and generalization of 13 mass-transfer equations for determining free water evaporation, *Hydrological Processes*, 11, 311-323, 10.1002/(SICI)1099-1085(19970315)11:3<311::AID-HYP446>3.0.CO;2-Y, 1997.

Sirois, A., and Barrie, L. A.: Arctic lower tropospheric aerosol trends and composition at Alert, Canada: 1980–1995, *Journal of Geophysical Research: Atmospheres*, 104, 11599-11618, 10.1029/1999JD900077, 1999.

Skov, H., Brooks, S. B., Goodsite, M. E., Lindberg, S. E., Meyers, T. P., Landis, M. S., Larsen, M. R. B.,



Jensen, B., McConville, G., and Christensen, J.: Fluxes of reactive gaseous mercury measured with a newly developed method using relaxed eddy accumulation, *Atmos. Environ.*, 40, 5452-5463, 10.1016/j.atmosenv.2006.04.061, 2006.

Slemr, F., Brunke, E.-G., Ebinghaus, R., Temme, C., Munthe, J., Wängberg, I., Schroeder, W., Steffen, A., and Berg, T.: Worldwide trend of atmospheric mercury since 1977, *Geophysical Research Letters*, 30, 10.1029/2003GL016954, 2003.

Spivakovsky, C. M., Logan, J. A., Montzka, S. A., Balkanski, Y. J., Foreman-Fowler, M., Jones, D. B. A., Horowitz, L. W., Fusco, A. C., Brenninkmeijer, C. A. M., Prather, M. J., Wofsy, S. C., and McElroy, M. B.: Three-dimensional climatological distribution of tropospheric OH: Update and evaluation, *Journal of Geophysical Research-Atmospheres*, 105, 8931-8980, 10.1029/1999jd901006, 2000.

Steffen, A., Schroeder, W., Bottenheim, J., Narayan, J., and Fuentes, J. D.: Atmospheric mercury concentrations: measurements and profiles near snow and ice surfaces in the Canadian Arctic during Alert 2000, *Atmos. Environ.*, 36, 2653-2661, 10.1016/S1352-2310(02)00112-7, 2002.

Steffen, A., Schroeder, W., Macdonald, R., Poissant, L., and Konoplev, A.: Mercury in the Arctic atmosphere: An analysis of eight years of measurements of GEM at Alert (Canada) and a comparison with observations at Amderma (Russia) and Kuujjuarapik (Canada), *Sci. Total Environ.*, 342, 185-198, 10.1016/j.scitotenv.2004.12.048, 2005.

Strode, S. A., Jaeglé, L., Selin, N. E., Jacob, D. J., Park, R. J., Yantosca, R. M., Mason, R. P., and Slemr, F.: Air-sea exchange in the global mercury cycle, *Global Biogeochem. Cycles*, 21, 10.1029/2006GB002766, 2007.

Sunderland, E. M., and Mason, R. P.: Human impacts on open ocean mercury concentrations, *Global Biogeochem. Cycles*, 21, 10.1029/2006GB002876, 2007.

Totten, L. A., Brunciak, P. A., Gigliotti, C. L., Dachs, J., Glenn, Nelson, E. D., and Eisenreich, S. J.:



Dynamic Air–Water Exchange of Polychlorinated Biphenyls in the New York–New Jersey Harbor Estuary, *Environmental Science & Technology*, 35, 3834–3840, 10.1021/es010791k, 2001.

Vieira, L. H., Achterberg, E. P., Scholten, J., Beck, A. J., Liebetrau, V., Mills, M. M., and Arrigo, K. R.: Benthic fluxes of trace metals in the Chukchi Sea and their transport into the Arctic Ocean, *Mar. Chem.*, 208, 43–55, 10.1016/j.marchem.2018.11.001, 2019.

Vihma, T., Jaagus, J., Jakobson, E., and Palo, T.: Meteorological conditions in the Arctic Ocean in spring and summer 2007 as recorded on the drifting ice station Tara, *Geophysical Research Letters*, 35, 10.1029/2008GL034681, 2008.

Vinogradova, A., and Polissar, A.: Elemental composition of the aerosol in the atmosphere of the central Russian Arctic (**in Russian**), *Izv Atmos Oceanic Phys*, 248–257 pp., 1995.

Walker, T. R., Young, S. D., Crittenden, P. D., and Zhang, H.: Anthropogenic metal enrichment of snow and soil in north-eastern European Russia, *Environ. Pollut.*, 121, 11–21, 10.1016/s0269-7491(02)00212-9, 2003.

Wang, F., Feng, T., Guo, Z., Li, Y., Lin, T., and Rose, N. L.: Sources and dry deposition of carbonaceous aerosols over the coastal East China Sea: Implications for anthropogenic pollutant pathways and deposition, *Environ. Pollut.*, 245, 771–779, doi.org/10.1016/j.envpol.2018.11.059, 2019.

Wängberg, I., Munthe, J., Berg, T., Ebinghaus, R., Kock, H. H., Temme, C., Bieber, E., Spain, T. G., and Stolk, A.: Trends in air concentration and deposition of mercury in the coastal environment of the North Sea Area, *Atmos. Environ.*, 41, 2612–2619, 10.1016/j.atmosenv.2006.11.024, 2007.

Wong, C. S. C., Duzgoren-Aydin, N. S., Aydin, A., and Wong, M. H.: Sources and trends of environmental mercury emissions in Asia, *Sci. Total Environ.*, 368, 649–662, doi.org/10.1016/j.scitotenv.2005.11.024, 2006.

Zhang, L., Gong, S., Padro, J., and Barrie, L.: A size-segregated particle dry deposition scheme for an atmospheric aerosol module, *Atmos. Environ.*, 35, 549–560, 10.1016/S1352-2310(00)00326-5, 2001.

Zhang, Y., and Tao, S.: Global atmospheric emission inventory of polycyclic aromatic hydrocarbons



(PAHs) for 2004, *Atmos. Environ.*, 43, 812-819, 10.1016/j.atmosenv.2008.10.050, 2009.

Zhulidov, A. V., Robarts, R. D., Pavlov, D. F., Kamari, J., Gurtovaya, T. Y., Merilainen, J. J., and Pospelov, I. N.: Long-term changes of heavy metal and sulphur concentrations in ecosystems of the Taymyr Peninsula (Russian Federation) North of the Norilsk Industrial Complex, *Environ. Monit. Assess.*, 181, 539-553, 10.1007/s10661-010-1848-y, 2011.



Figure caption list

Figure 1. Locations of investigated islands for soil sampling and trajectory of the vessel in the Russian Arctic.

Figure 2. Occurrence of heavy metals. Results show the concentrations of heavy metals in the (a) gas phase, (b) aerosol phase, (c) and dissolved water phase. Colored bars show the sum of nine quantified metals. The number at the bottom of the legend bars represent the concentration scale as same as Figure 3-7.

Figure 3. Measured atmosphere–ocean exchange of heavy metals. (a) Fluxes of dry deposition for nine heavy metals; (b) fluxes of net diffusive air–water exchange for Hg. In panel (a), colored bars represent the sum of nine heavy metals. In panel (b), downward bars represent the net deposition into the ocean, and upward bars represent the net volatilization of Hg.

Figure 4. Wet deposition of (a) heavy metals and (b) PAH fluxes. The measured wet deposition of heavy metals and PAHs occurred during the eight snow events encountered during the vessel expedition.

Figure 5. Occurrence of PAHs in the Russian Arctic Ocean. Concentrations of PAHs in the (a) gas phase, (b) aerosol phase, and (c) dissolved water phase. Color bars indicate the sum of 35 PAHs, where each PAH corresponds to the bottom legend (colors range from red for the heaviest molecular weight PAHs to green for the lightest molecular weight PAHs).

Figure 6. Measured atmosphere–ocean exchange of PAHs. (a) Dry deposition fluxes for the 35 measured PAHs; (b) net diffusive air–water exchange fluxes (all net deposition into the ocean) for fluoranthene, tetramethylphenanthrene, trimethylphenanthrene, and dibenzothiophene. Color bars indicate the sum of the 35 quantified compounds, and each color represents the individual PAHs in the bottom legend (colors range from red for the heaviest molecular weight PAHs to green for the lightest molecular weight PAHs).

Figure 7. Atmospheric degradation of PAHs. Estimated fluxes of degraded PAHs in the gas phase following reaction with OH radicals.

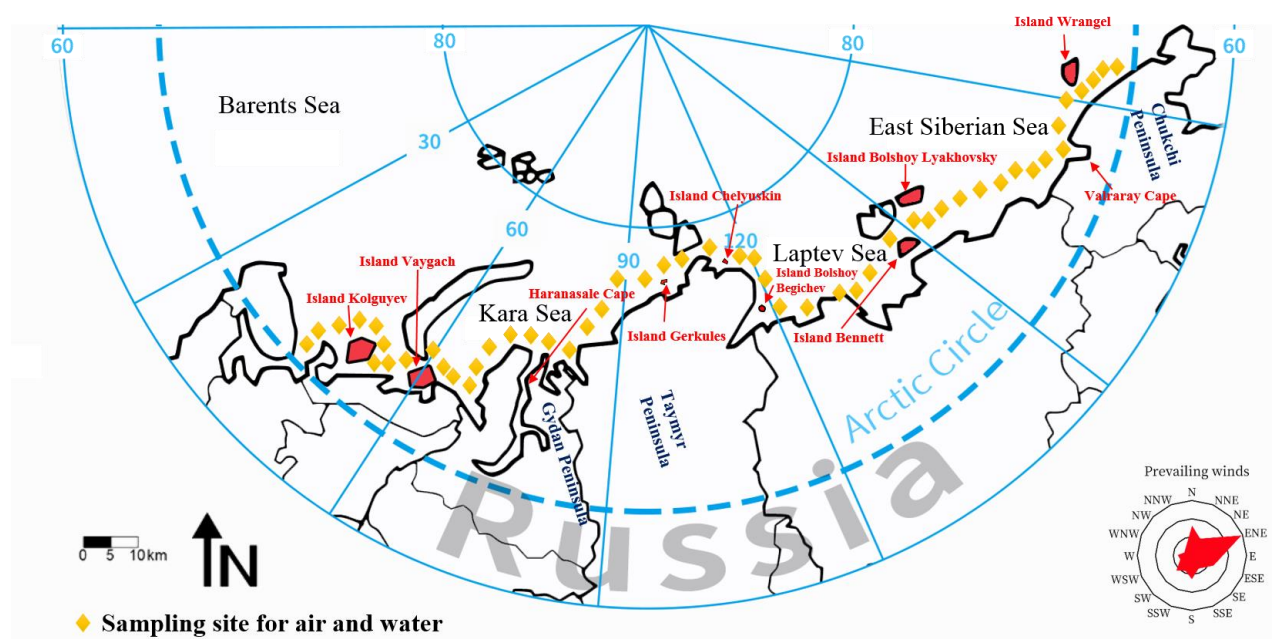


Figure 1.

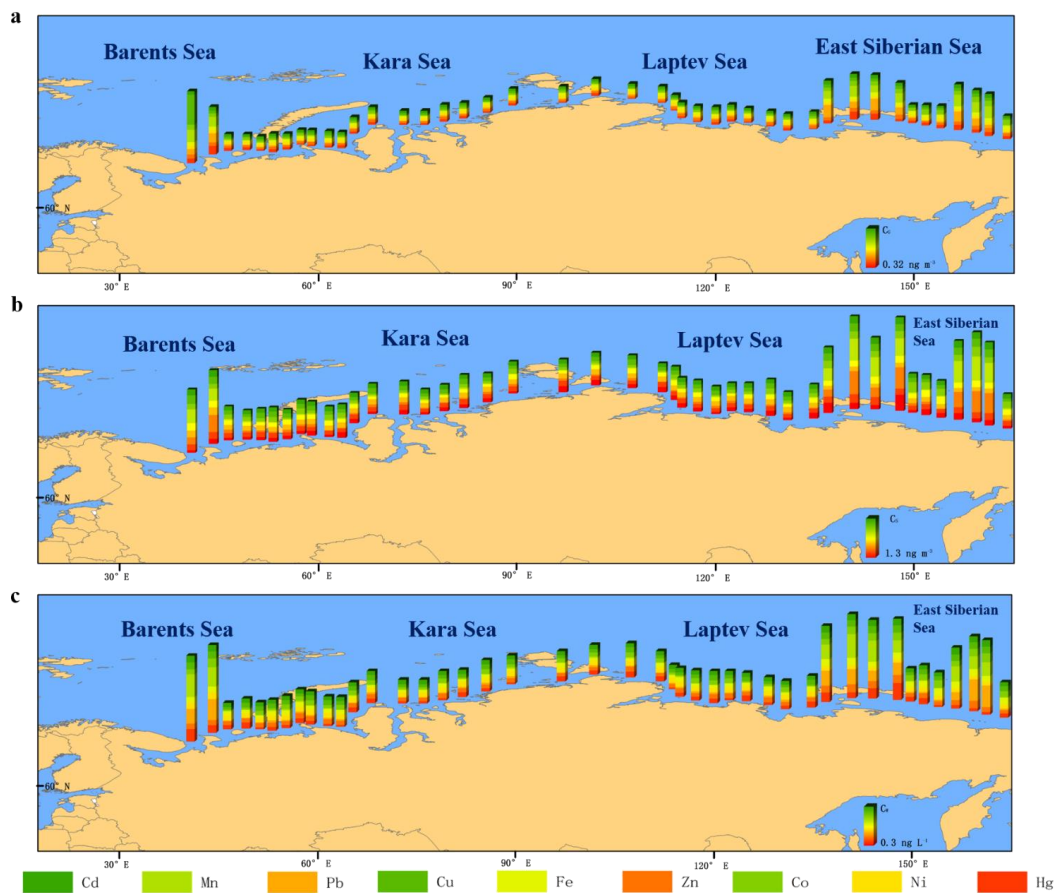


Figure 2.

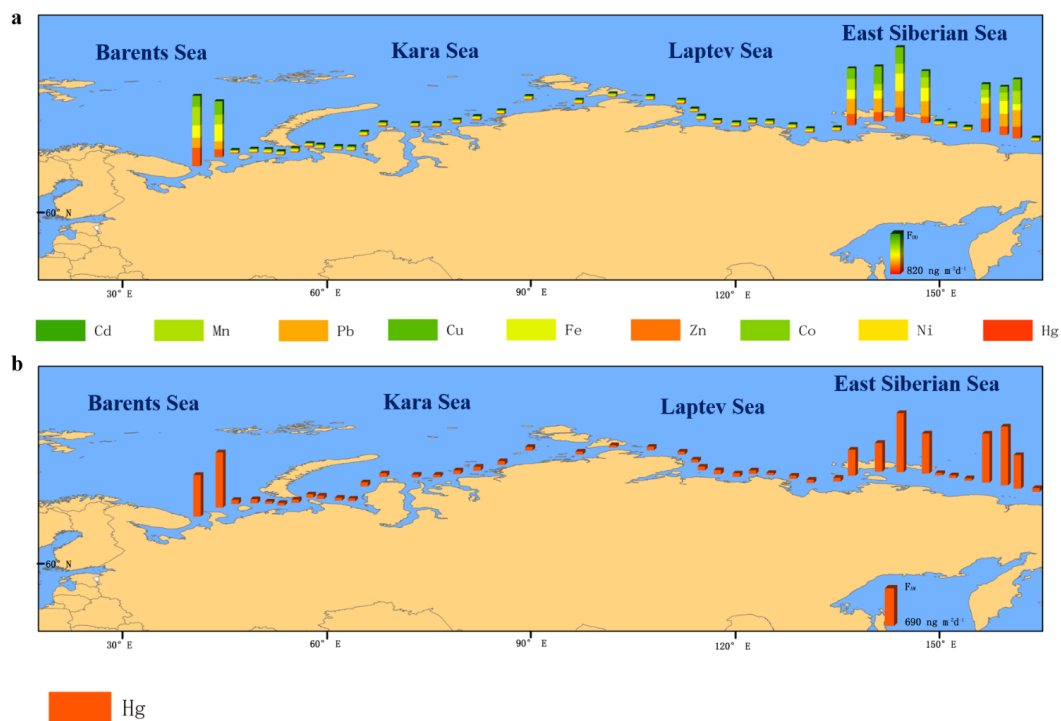


Figure 3.

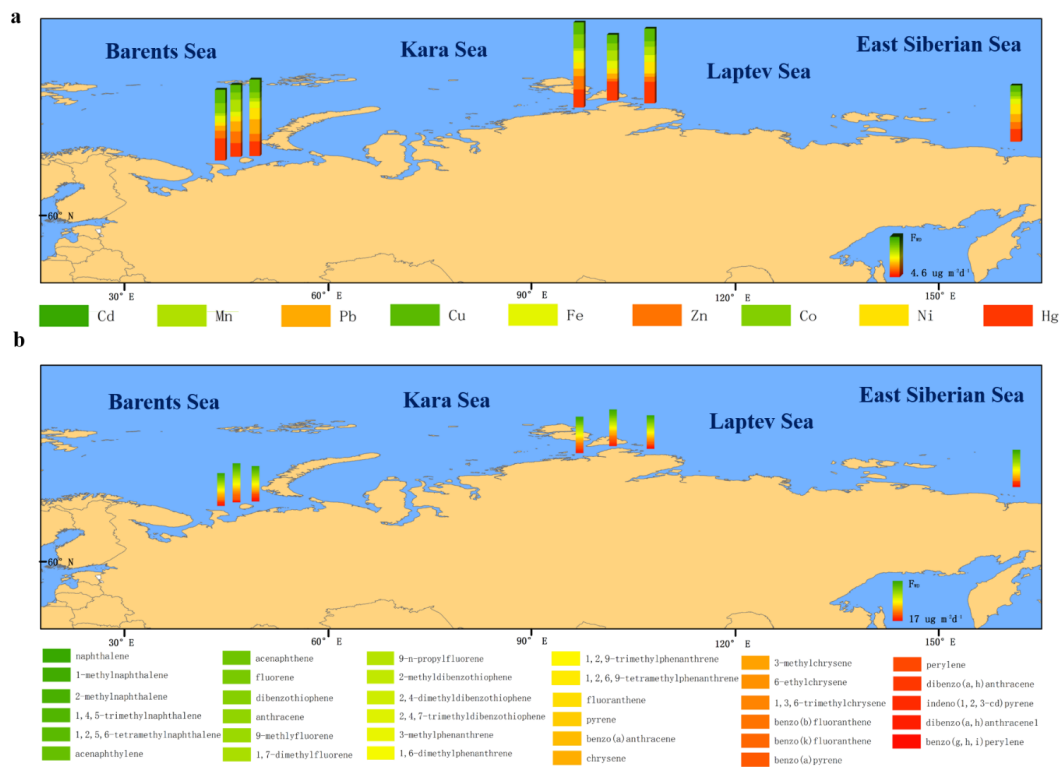


Figure 4.

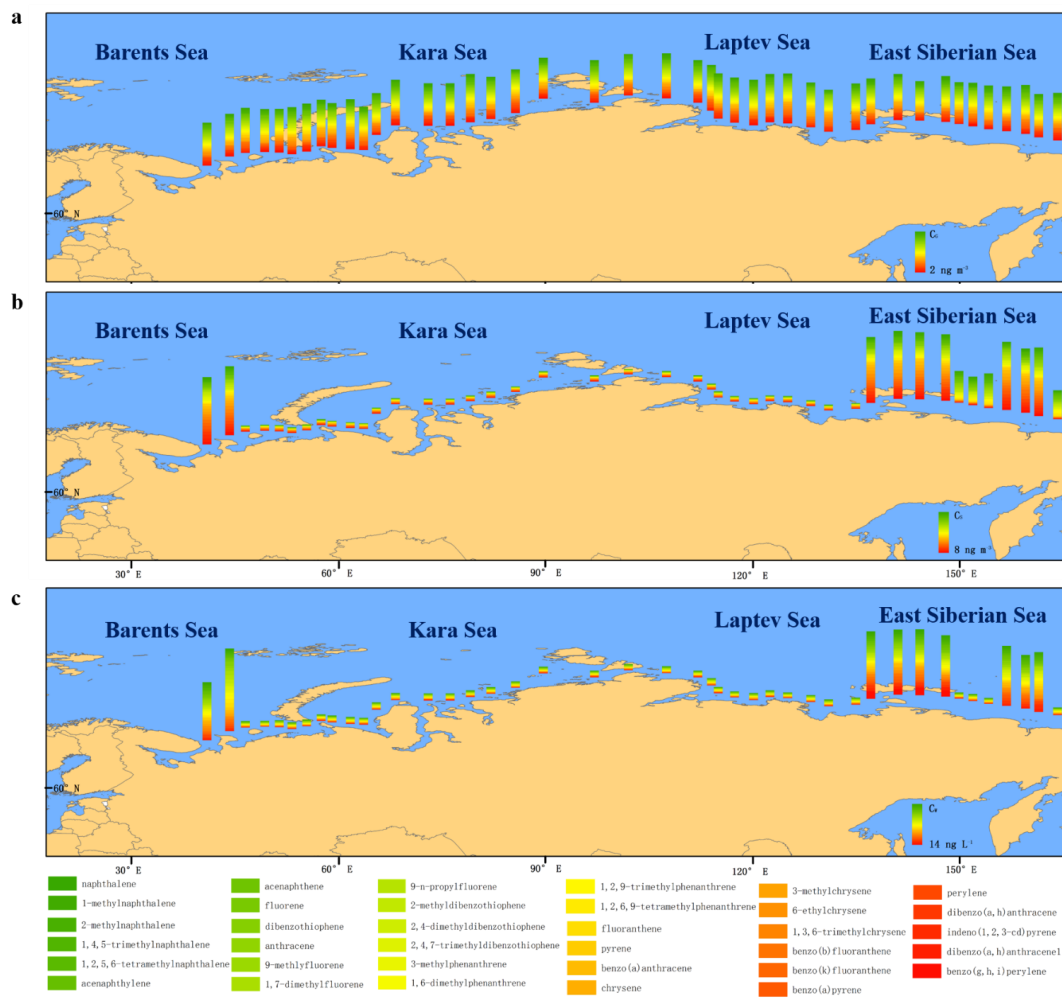


Figure 5.

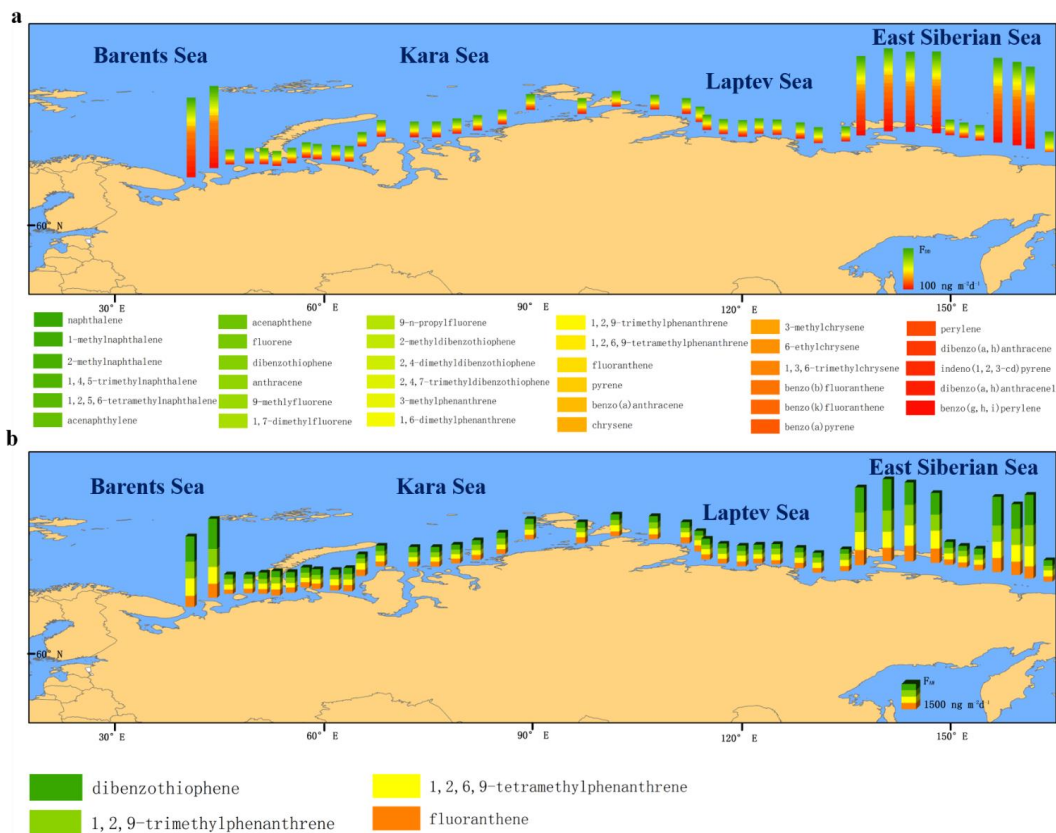


Figure 6.

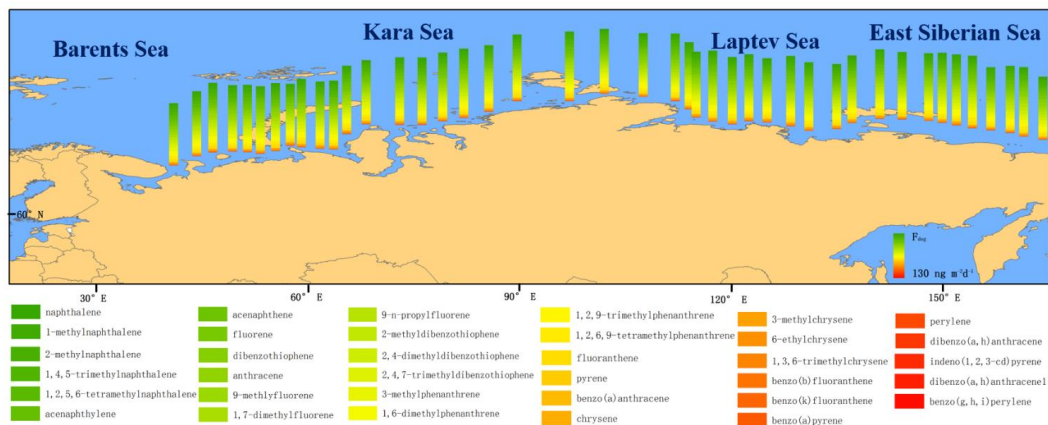


Figure 7.